



Published in final edited form as:

Nat Rev Mol Cell Biol. ; 12(11): 749–756. doi:10.1038/nrm3212.

Imaging the coordination of multiple signaling activities in living cells

Christopher M. Welch^{1,*}, Hunter Elliott^{2,*}, Gaudenz Danuser², and Klaus M. Hahn¹

¹Department of Pharmacology and Lineberger Cancer Center, University of North Carolina at Chapel Hill, Chapel Hill, North Carolina 27599, USA

²Department of Cell Biology, Harvard Medical School, Boston, Massachusetts 02115, USA

Preface

Cellular signal transduction occurs in complex and redundant interaction networks that are best examined at the level of single cells by simultaneously monitoring the activation dynamics of multiple components. Recent advances in biosensor technology have made it possible to visualize and quantify the activation of multiple network nodes in the same living cell. The precision and scope of this approach has been greatly extended by novel computational approaches to determine the relationships between different networks, studied in separate cells.

Introduction

Methods such as phospho-proteomics¹, protein-protein interaction studies² and gene expression profiling³ allow analysis of signaling networks via the simultaneous observation of every pathway component. However, these methods average information over many cells and do not take into account cell-to-cell heterogeneity, which has been shown to play key roles in the function of signaling networks^{4–6}. Flow cytometry allows the measurement of signaling at the single cell level⁷ but, similar to proteomic methods, temporal information is available only as a many-cell average, and spatial information is either completely absent or at very coarse levels, such as membrane and organelle compartmentalization.

A tool chest of fluorescent proteins emitting from the ultra violet (UV) to the near infrared have made it possible to simultaneously visualize the subcellular dynamics of multiple proteins in the same living cell — a technique referred to as experimental multiplexing. Such ‘multiplexed imaging’, which can reveal the coordination of two or more subcellular structures, is now routinely exploited to study, for example, the interactions of cytoskeletal fibers^{8,9}, the transient coupling of adhesion molecules and cytoskeleton flows¹⁰, and the choreography of protein recruitment to endocytic sites at the plasma membrane¹¹. In contrast, the subcellular coordination of the signaling events that regulate these dynamics has remained considerably more obscure. In some cases, a single signaling activity can be visualized together with the dynamics of subcellular structures, but this has until recently been restricted largely to second messengers, for example, fluorescent chelators that report ion concentrations^{12,13}, or fluorescently tagged domains that bind accumulations of lipid second messengers^{14,15} or mark cellular structures¹⁶. The study of the coordinated activation of multiple signaling proteins has been hindered by formidable technical hurdles. These obstacles have been recently overcome by two very different but complementary

Address correspondence to: Gaudenz_Danuser@hms.harvard.edu, khahn@med.unc.edu.
*these authors contributed equally to this review

approaches — the development of powerful new biosensors and the development of computational multiplexing.

To understand the spatiotemporal dynamics of signaling events, it is generally not sufficient to simply follow the changing localization of proteins. Signaling proteins interact with downstream targets only in specific ‘activated’ states. Therefore, to dissect the mechanism of signal transduction it is necessary to monitor protein localization and activation. Biosensors have been devised to report protein activation states, usually relying on Förster resonance energy transfer (FRET) readouts of a conformational change or protein interaction^{17, 18}. Due to the availability of fluorescent proteins spanning much of the visible spectrum, FRET-based biosensors can now be built using fluorescent proteins with orthogonal wavelengths, enabling the imaging of two biosensors in the same cell. Furthermore, a deeper understanding of fluorescent proteins has permitted the design of biosensors that respond directly to endogenous signaling molecules, without the need to use two fluorescent proteins. These experimental multiplexing approaches may ultimately enable us to visualize the activities of three and four signaling molecules at the same time.

However, even with these improved designs, only a limited number of biosensors can be introduced into one cell. In addition, multi-spectral imaging and introduction of multiple exogenous proteins is often accompanied by increased phototoxicity and the perturbation of cell physiology. Ideally one could study the dynamics of each protein species separately in different cells and subsequently relate them to each other via correlation with a common fiduciary event that occurs in each cell. Indeed, this approach has been applied, to study the timing of signaling events during phagocytosis and wound closure^{19–21}. However, many cellular functions display stochastic behaviors, resulting in a wide range of heterogeneous, less stereotypical signaling patterns. In this case, establishing the relationships between signaling activities that are not all observed in the same cell is quite challenging. Recent work by several labs has begun to break through this barrier. It has been shown that spatiotemporal relationships between any two co-observed cellular activities can be extracted from their constitutive, basal fluctuations^{22–24}. It has also been shown that, when measuring the relationships between two pairs of activities in different cells, with one activity in common between the pairs, it is possible to predict the spatiotemporal relationships among all of the individual activities, even when they are observed in different cells²². This process has been referred to as computational multiplexing in order to distinguish it from experimental multiplexing. Although computational multiplexing is still in its very early days, it may ultimately become the technology of choice for reconstructing complex pathways with many component activities. Importantly, the concept of computational multiplexing relies on concurrent measurements of activities in pairs, triplets, or even quadruplets. The more relations that can be extracted through direct observation in single experiments, the more robust will be the computationally inferred relations between signaling components. Therefore, advances in experimental multiplexing will lay the groundwork for advances in computational multiplexing. The goal of this Innovation is to outline the current state of both experimental and computational multiplexing, and to project their joint potential for the analysis of signal transduction at the single cell level.

Experimental multiplexing

The great majority of experiments studying multiple signaling nodes in the same living cell have been accomplished by combining genetically encoded FRET biosensors, the most tractable and commonly used type of biosensor. These have been extended to multiplexing primarily through development of new FRET pairs with orthogonal wavelengths, and advances in instrumentation and techniques to enhance sensitivity. Both are important, as the primary limitation to experimental multiplexing appears to be the ability of living cells

to tolerate multiple exogenous reporter molecules. A host of other developing approaches show promise, some requiring the use of only one fluorophore to monitor each activity, or with significantly reduced cell perturbation.

Multiplexing with genetically encoded FRET

Although several different FRET pairs have been used to construct biosensors (for example, BFP/CFP, EGFP/DsRed and CFP/YFP), the CFP/YFP pair has proven most useful in multiplexing, due to its superior fluorescence properties and excitation/emission wavelengths that are compatible with other fluorophores. The development of orange and red proteins spectrally distinct from CFP and YFP²⁵, and the subsequent improvement in their photostability and brightness^{26, 27}, have provided compatible FRET pairs for multiplexing (See Figure 1 and Table 1). In an impressive example of multiparameter imaging, Piljic *et al.* studied two, three, and four activities simultaneously²⁸. These authors used two CFP/YFP FRET probes (a Ca²⁺/Calmodulin-dependent kinase II sensor and a membrane-bound PKC sensor) together with an orthogonal mOrange/mCherry FRET pair in a sensor for the assembly of Annexin4 (a calcium-dependent phospholipid binding protein). This enabled ratiometric, spatially resolved FRET imaging. By restricting themselves to monitoring only the FRET intensity changes of the Annexin4 biosensor, the kinetics of annexin assembly into a trimer, which is facilitated by calcium influx, could be followed together with Fura Red to sense Ca²⁺ level changes, and these two activities could then be correlated with the activities of CaMKII and PKC signaling in live cells to determine the time sequence of Ca²⁺ influx, cellular signaling, and the resultant Annexin4 assembly.

Rather than use FRET pairs compatible with CFP/YFP, Ai *et al.*²⁹ generated new fluorophores and combined mTeal/YFP with mAmetrine/tdTomato to image both nucleus-targeted and nucleus-excluded caspase-3 activity within the same cell. mAmetrine is a unique fluorophore with a large Stokes shift and a violet-shifted excitation spectrum; this allows its effective separation from mTeal. Similarly, T-Sapphire/DsRed has also been used in combination with a CFP/YFP FRET pair, to detect cGMP concentrations³⁰. But, since T-Sapphire has an excitation spectrum similar to CFP and a large Stokes shift that allows it to FRET with DsRed, this fluorophore permits simultaneous excitation of two spectrally separable FRET pairs. Recently, “ultramarine” fluorophores with excitation/emission in the violet have emerged^{31, 32}. These require cell irradiation with more ‘toxic’ UV light, but may enable simultaneous imaging of three FRET biosensors when paired with another violet-shifted fluorophore such as BFP.

Imaging fluorescence lifetime rather than fluorescence intensity provides important advantages for FRET multiplexing. FRET quenches donor fluorescence, thus affecting donor fluorescence lifetime. Unlike intensity measurements, the donor lifetime is insensitive to sources of artifacts such as uneven illumination, subcellular variation in probe concentration, or cell geometry (reviewed in⁴⁵⁻⁴⁷ and elsewhere). Fluorescence lifetime imaging (FLIM) expands the number of usable FRET pairs for multiplexing because only effects on donor fluorescence are measured. Thus, the same acceptor can be used for two different donors⁴⁸, and the choice of available proteins can be extended to include non-fluorescent acceptors, such as dkYFP⁴⁹. With current technology, FLIM does incur either reduced temporal or spatial resolution relative to widefield imaging, and not all donor fluorophores are useful for FLIM imaging. However, donor fluorophores and fluorophore combinations with potential for FLIM multiplexing have been described⁵⁰⁻⁵⁴: mRFP/GFP, mStrawberry/GFP, mRFP/Venus, mStrawberry/Venus, and mDarkVenus/mGFP were all found to be comparable for FLIM imaging of CaMKII using variants of the Camui sensor, a FRET-based sensor of CaMKII activity.

On the horizon

FRET can also be accomplished using organic dyes, quantum dots, and other inorganic fluorophores. Compared to fluorescent proteins these fluorescent markers provide superior brightness and photostability^{33, 34}, but they are not genetically encoded. Brightness and photostability are important for multiplexing, as they determine how much biosensor must be used in a cell to generate a robust signal. This is especially important when multiple biosensors are loaded in the same cell, as more biosensors increase cellular perturbation. In a recent study, a FRET biosensor for RhoA was combined with a Cdc42 biosensor based on an environment-sensing dye. The dye was attached to a protein domain that bound selectively to activate Cdc42²². Upon binding activated Cdc42 the dye on the biosensor underwent a shift in fluorescence, revealing the localization of Cdc42 activity. This design substantially reduced the concentration of biosensor needed, as it enabled the sensing of endogenous Cdc42, and used direct excitation of a bright dye. However, despite their greater sensitivity and ability to operate at lower intracellular concentrations, non-genetic biosensors are rarely used because they have to be loaded into cells via cumbersome methods such as microinjection or electroporation. Recent approaches to attach dyes to proteins *in vivo* show promise for harnessing the advantages of non-genetic fluorophores³⁵.

Signaling behaviors have also been reported by using only a single fluorescent protein, rather than by FRET. This facilitates experimental multiplexing as each biosensor uses a smaller portion of the wavelength spectrum. These approaches include fluorescent proteins that respond to ions, pH, voltage, or reactive oxygen species¹⁸. In bimolecular fluorescence complementation (BiFc), a fluorescent protein is split into two nonfluorescent halves, each linked to a different signaling protein. When the two signaling proteins bind, they bring the two halves of the fluorescent protein together, generating fluorescence. In some applications, one half of the fluorescent protein can combine with two different second halves^{36–40}, each generating a unique color, including a far red version of the split protein, mLumin⁴¹. This technique is very sensitive because the signal is created over a ‘dark’ background. However, the interaction of the two halves is currently irreversible and the fluorescence forms with relatively slow kinetics. FRET between identical fluorophores, observed through effects on fluorescence polarization anisotropy, has been used to study receptor oligomerization, or protein aggregation, without the need for two different fluorophores^{42–44}.

Important strides in experimental multiplexing will have to come from improved sensitivity in biosensor imaging, as toxicity and cell perturbation are important issues when studying low abundance signaling proteins. Several papers have addressed how the relative concentrations of biosensors and endogenous proteins or molecules affect cell behavior^{55–61}; some have proposed that sensors can be applied to specific, well selected proteins to reveal the behavior of larger networks, ideally proteins of high concentration less likely to be perturbed by introducing biosensors^{62–64}.

Computational multiplexing

Progress in biosensor design and the spectral decomposition of images, and improvements in filters and instrumentation, will steadily increase the number of simultaneously observable molecular activities. However, deriving a complete analysis of pathway states by studying all of the components in the same cell is unlikely in the foreseeable future. Thus, methods are needed that complement the direct imaging of multiplexed biosensors with the ability to integrate data from independent experiments into a comprehensive pathway model. These methods are collectively referred to as ‘computational multiplexing (Figure 2). Several challenges must be overcome when implementing computational multiplexing approaches. First, the integration of data from multiple experiments implies that the properties of the

studied pathway, that is, the hierarchy of pathway components and the kinetics of information transfer between them, do not change between experiments. Practically, this means that the cell state and the environmental conditions are held identical between experiments, for example, by using clonal cell populations. Second, even then, the activation dynamics of the pathway will vary from cell to cell. Therefore, methods for data integration are required that identify from variable cell responses a canonical, cell-invariant representation of the pathway. Third, the spatiotemporal coupling of biosensor activities, whether observed in the same or separate experiments, usually results from nonlinear pathways, the feedback and feedforward relations of which are unknown *a priori*. Therefore, data integration must be combined with mathematical approaches for network inference. In this section we discuss strategies towards fulfilling these requirements, with reference to studies where the computational multiplexing of biosensors has provided insights into signaling pathways with sub-cellular resolution.

A need for conserved experimental conditions

The conservation of the fundamental pathway properties is an implicit assumption made by every investigator who repeats an experiment to average the responses of multiple cells. This is no different with computational multiplexing. However, when combining data from experiments probing different aspects of a pathway with different biosensors, this assumption must be thoroughly validated. The expression or microinjection of a biosensor can shift the pathway properties. To control for such effects, the reproducibility of a cell function related to the studied pathway must be tested for each biosensor that is expressed, over a range of concentrations. For example, for pathways that regulate cell morphogenesis, cell morphology or morphodynamics are excellent measures against which to identify probe-induced biases. These measurements can be accomplished either by manual inspection or, ideally, by quantitative morphological⁶⁵ or morphodynamic⁶⁶ analyses.

A common fiduciary mark between experiments

To determine the spatiotemporal relations between activities monitored in independent experiments, spatial and temporal fiduciaries are required that are common between experiments and invariant to changes in cell morphology and cell behavior. Temporal fiduciaries can be defined by the acute stimulation or inhibition of a pathway⁶⁷. By applying the same intervention protocol across multiple experiments, different biosensor activities can be aligned in time to deduce a response hierarchy. Similarly, spatiotemporal fiduciaries can be defined by spatially limiting the acute stimulation or inhibition of a pathway. Numerous approaches have been proposed to achieve this while monitoring downstream signaling responses, including mechano-stimulation of cells by micro-spheres^{68, 69} or photo-switchable reagents^{70, 71}.

Recently, two studies independently established the concept of inferring a response hierarchy from constitutive fluctuations in the activity of biosensors. Time shifts between signaling events were determined by temporal and spatial cross-correlation between the activation of two biosensors, and/or between the activation of one biosensor and spontaneous fluctuations in cell morphology^{22, 24} (Fig. 3). There are several key advantages to this strategy as compared to the acute stimulation or inhibition of a pathway. First, acute interventions may over stimulate or over perturb pathways. As a result, the kinetics and response hierarchies deduced from these experiments may reflect a pathway that operates far outside the range of normal physiology. As well as avoiding this problem, the second advantage of analyzing constitutive fluctuations is that this permits a dense mapping of spatial gradients in signaling hierarchies. For example, the study by Machacek *et al.*²², of the coordination of Rho GTPases during cell protrusion, suggested that not only is the activation of Rac1 delayed by ~40 s relative to the activation of RhoA, but it is also shifted in space by

~2 microns. While RhoA is activated at the cell edge, Rac1 is activated behind the cell edge, possibly in growing nascent adhesions. It would be very tedious to derive such predictions of the spatiotemporal organization of pathways from a few scarcely distributed interventions. Third, in concept fluctuation analysis is readily scalable to pathways involving a very large number of components. To make use of this potential, pairwise cross-correlation analysis must be replaced by more sophisticated mathematical tools that integrate, from multiple experiments, the image fluctuation sequences of partially overlapping sets of component activities.

Appropriate spatiotemporal sampling

The possibility of exploiting constitutive fluctuations to infer the response hierarchy and kinetics of pathways relies on the proper sampling of biosensor activities. The sampling resolution in time must be a few times faster than the time scale of information transmission through the pathway. Otherwise, the fluctuation sequences of different pathway components are decoupled. The sampling resolution in space must be high enough to preclude the averaging of adjacent yet independent pathway events. On the other hand, some averaging may be desirable to reduce measurement noise in the fluctuations. As illustrated in Fig. 4, the required time and length scales for sampling signaling activities can be deduced from the autocorrelation functions of the cellular outputs of the pathway; that is, in the example shown, cell protrusion dynamics.

Reconstructing the pathway hierarchy

Until recently, studies involving multiple biosensor activities have used pairwise cross-correlation to infer the relations between pathway components^{22, 72}. Component pairs, the correlation of which does not reach a defined significance level are considered disconnected in the pathway, whereas pairs with a significant correlation are considered directly or indirectly coupled. These pairwise analysis methods, though simple, have major limitations. First, as mentioned above, they do not provide the means for a rigorous integration of multiple experiments in one model. Second, cross-correlation approaches break down in the presence of strong feedback and/or feedforward interactions between pathway components. Third, although temporal cross-correlation generates some evidence for the hierarchy of activation, by determining what comes first and what comes second, it cannot define causal relations between pathway components. Two unconnected activities may be correlated with each other simply because they are downstream of the same activity. Much work is underway to identify causal networks from common fluctuations in gene expression profiles or proteomic data^{7, 73, 74}. Some of these frameworks even have been expanded to non-simultaneously observed data⁷⁵. In contrast to genomic and proteomic data sets, however, biosensor images offer more finely resolved information about the dynamics and sub-cellular localization of pathway activities. While this additional information will greatly enhance the inference of the pathway hierarchy, it introduces new challenges for the design of algorithms that integrate data from a sequence of different experiments.

Conclusion

In summary, new biosensor designs with extended spectral properties and vastly increased sensitivity have opened exciting opportunities for signal transduction research. It has become possible to simultaneously monitor two or three signaling activities, and enhanced sensitivity permits the analysis of highly localized constitutive pathway fluctuations. This in turn enables the use of powerful statistical formalisms for the integration of multiple experiments and for the inference of hierarchy in signaling networks. Conceptually, this has brought us to the point where complex pathways with many components and redundant and nonlinear cascades can be studied in living cells under fairly physiological conditions.

However, to turn this concept into a routine tool for the cell biologist, developments on the horizon will play a major role. To apply computational multiplexing by relying on combinations of biosensors in the same cell, issues of cell perturbation will become even more important in biosensor design. To overcome these issues, biosensors must be developed with enhanced sensitivity that enables their effective use at lower concentrations; this may stem from brighter fluorophores, direct excitation, and improvements in instrumentation. Designs responding to endogenous proteins will also reduce cell perturbation. Novel approaches to decrease the spectral bandwidth of each biosensor will increase the number of activities that can be imaged simultaneously, and might include the development of FLIM with an enhanced signal to noise ratio, biosensors that are based on single fluorophores, and spectral deconvolution imaging. As computational multiplexing provides us with an ability to multiplex an essentially unlimited number of signaling molecules, our ability to produce biosensors will become a bottleneck. Soon, biosensors will not need to be based on naturally occurring domains or substrates with the desired specificity, but can be generated via high throughput screening of engineered scaffolds⁷⁶.

Supplementary Material

Refer to Web version on PubMed Central for supplementary material.

Glossary

<i>Orthogonal wavelengths</i>	Emission or excitation wavelengths of two fluorescent probes are sufficiently different to be imaged separately
<i>Ratiometric imaging</i>	Biosensors can be designed so that the ratio of emission or excitation at two different wavelengths reflects the biological activity being measured. This ratio is independent of the biosensor's fluorescence intensity, so eliminates effects of cell thickness, uneven biosensor distribution, uneven illumination etc
<i>Stokes shift</i>	Difference between the excitation and emission wavelengths of a fluorescent probe
<i>Quantum dots</i>	Small semiconductor crystals that emit light of a longer wavelength upon excitation with a shorter wavelength, akin fluorophores
<i>Fluorescence polarization anisotropy</i>	This technique measures the rotational diffusion of fluorophores by measuring the difference in the polarization of excitation and emission light. Changes in fluorescence polarization anisotropy indicate changes in the rotational diffusion of molecules induced by their interactions with other molecules
<i>Spectral image decomposition</i>	Mathematical technique to separate the contribution of multiple fluorophore species to the image signal at a certain wavelength. This allows the separation of the signals of fluorophores with overlapping emission spectra

References

1. Olsen JV, et al. Global, in vivo, and site-specific phosphorylation dynamics in signaling networks. *Cell*. 2006; 127:635–648. [PubMed: 17081983]
2. Barrios-Rodiles M, et al. High-throughput mapping of a dynamic signaling network in mammalian cells. *Science*. 2005; 307:1621–1625. [PubMed: 15761153]
3. Margolin AA, et al. ARACNE: An algorithm for the reconstruction of gene regulatory networks in a mammalian cellular context. *Bmc Bioinformatics*. 2006; 7

4. Spencer SL, Gaudet S, Albeck JG, Burke JM, Sorger PK. Non-genetic origins of cell-to-cell variability in TRAIL-induced apoptosis. *Nature*. 2009; 459:428–U144. [PubMed: 19363473]
5. Colman-Lerner A, et al. Regulated cell-to-cell variation in a cell-fate decision system. *Nature*. 2005; 437:699–706. [PubMed: 16170311]
6. Cohen-Saidon C, Cohen AA, Sigal A, Liron Y, Alon U. Dynamics and Variability of ERK2 Response to EGF in Individual Living Cells. *Molecular Cell*. 2009; 36:885–893. [PubMed: 20005850]
7. Sachs K, Perez O, Pe'er D, Lauffenburger DA, Nolan GP. Causal Protein-Signaling Networks Derived from Multiparameter Single-Cell Data. *Science*. 2005; 308:523–529. [PubMed: 15845847]
8. Salmon WC, Adams MC, Waterman-Storer CM. Dual-wavelength fluorescent speckle microscopy reveals coupling of microtubule and actin movements in migrating cells. *J Cell Biol*. 2002; 158:31–7. [PubMed: 12105180]
9. Schaefer AW, et al. Coordination of actin filament and microtubule dynamics during neurite outgrowth. *Dev Cell*. 2008; 15:146–62. [PubMed: 18606148]
10. Hu K, Ji L, Applegate KT, Danuser G, Waterman-Storer CM. Differential transmission of actin motion within focal adhesions. *Science*. 2007; 315:111–5. [PubMed: 17204653]
11. Taylor MJ, Perrais D, Merrifield CJ. A high precision survey of the molecular dynamics of mammalian clathrin-mediated endocytosis. *PLoS Biol*. 9:e1000604. [PubMed: 21445324]
12. Harbeck MC, et al. Simultaneous optical measurements of cytosolic Ca²⁺ and cAMP in single cells. *Sci STKE*. 2006:pl6. [PubMed: 16985238]
13. Wier WG, Rizzo MA, Raina H, Zacharia J. A technique for simultaneous measurement of Ca²⁺, FRET fluorescence and force in intact mouse small arteries. *J Physiol*. 2008; 586:2437–43. [PubMed: 18372302]
14. Tengholm A, Teruel MN, Meyer T. Single cell imaging of PI3K activity and glucose transporter insertion into the plasma membrane by dual color evanescent wave microscopy. *Sci STKE*. 2003:PL4. [PubMed: 12582202]
15. Tanimura A, Nezu A, Morita T, Turner RJ, Tojyo Y. Fluorescent biosensor for quantitative real-time measurements of inositol 1,4,5-trisphosphate in single living cells. *J Biol Chem*. 2004; 279:38095–8. [PubMed: 15272011]
16. Kitano M, Nakaya M, Nakamura T, Nagata S, Matsuda M. Imaging of Rab5 activity identifies essential regulators for phagosome maturation. *Nature*. 2008; 453:241–5. [PubMed: 18385674]
17. VanEngelenburg SB, Palmer AE. Fluorescent biosensors of protein function. *Curr Opin Chem Biol*. 2008; 12:60–5. [PubMed: 18282482]
18. Newman RH, Fosbrink MD, Zhang J. Genetically encodable fluorescent biosensors for tracking signaling dynamics in living cells. *Chem Rev*. 111:3614–66. [PubMed: 21456512]
19. Hoppe AD, Swanson JA. Cdc42, Rac1, and Rac2 display distinct patterns of activation during phagocytosis. *Mol Biol Cell*. 2004; 15:3509–19. [PubMed: 15169870]
20. Swanson JA, Hoppe AD. The coordination of signaling during Fc receptor-mediated phagocytosis. *J Leukoc Biol*. 2004; 76:1093–103. [PubMed: 15466916]
21. Vaughan EM, Miller AL, Yu HY, Bement WM. Control of local Rho GTPase crosstalk by Abr. *Curr Biol*. 21:270–7. [PubMed: 21295482]
22. Machacek M, et al. Coordination of Rho GTPase activities during cell protrusion. *Nature*. 2009; 461:99–103. [PubMed: 19693013]
23. Ji L, Lim J, Danuser G. Fluctuations of intracellular forces during cell protrusion. *Nature Cell Biology*. 2008; 10:1393–U38.
24. Tsukada Y, et al. Quantification of local morphodynamics and local GTPase activity by edge evolution tracking. *PLoS Comput Biol*. 2008; 4:e1000223. [PubMed: 19008941]
25. Matz MV, et al. Fluorescent proteins from nonbioluminescent Anthozoa species. *Nat Biotechnol*. 1999; 17:969–73. [PubMed: 10504696]
26. Shaner NC, et al. Improved monomeric red, orange and yellow fluorescent proteins derived from *Discosoma* sp. red fluorescent protein. *Nat Biotechnol*. 2004; 22:1567–72. [PubMed: 15558047]
27. Shaner NC, et al. Improving the photostability of bright monomeric orange and red fluorescent proteins. *Nat Methods*. 2008; 5:545–51. [PubMed: 18454154]

28. Piljic A, Schultz C. Simultaneous recording of multiple cellular events by FRET. *ACS Chem Biol*. 2008; 3:156–60. [PubMed: 18355004]
29. Ai HW, Hazelwood KL, Davidson MW, Campbell RE. Fluorescent protein FRET pairs for ratiometric imaging of dual biosensors. *Nat Methods*. 2008; 5:401–3. [PubMed: 18425137]
30. Niino Y, Hotta K, Oka K. Blue fluorescent cGMP sensor for multiparameter fluorescence imaging. *PLoS One*. 2010; 5:e9164. [PubMed: 20161796]
31. Niino Y, Hotta K, Oka K. Simultaneous live cell imaging using dual FRET sensors with a single excitation light. *PLoS One*. 2009; 4:e6036. [PubMed: 19551140]
32. Tomosugi W, et al. An ultramarine fluorescent protein with increased photostability and pH insensitivity. *Nat Methods*. 2009; 6:351–3. [PubMed: 19349978]
33. Sapsford KE, Berti L, Medintz IL. Materials for fluorescence resonance energy transfer analysis: beyond traditional donor-acceptor combinations. *Angew Chem Int Ed Engl*. 2006; 45:4562–89. [PubMed: 16819760]
34. Pertz O, Hahn KM. Designing biosensors for Rho family proteins—deciphering the dynamics of Rho family GTPase activation in living cells. *Journal of Cell Science*. 2004; 117:1313–1318. [PubMed: 15020671]
35. Hinner MJ, Johnsson K. How to obtain labeled proteins and what to do with them. *Curr Opin Biotechnol*. 21:766–76. [PubMed: 21030243]
36. Hu CD, Kerppola TK. Simultaneous visualization of multiple protein interactions in living cells using multicolor fluorescence complementation analysis. *Nature Biotechnology*. 2003; 21:539–545.
37. Kodama Y, Wada M. Simultaneous visualization of two protein complexes in a single plant cell using multicolor fluorescence complementation analysis. *Plant Mol Biol*. 2009; 70:211–7. [PubMed: 19219406]
38. Vidi PA, Chemel BR, Hu CD, Watts VJ. Ligand-dependent oligomerization of dopamine D(2) and adenosine A(2A) receptors in living neuronal cells. *Mol Pharmacol*. 2008; 74:544–51. [PubMed: 18524886]
39. Grinberg AV, Hu CD, Kerppola TK. Visualization of Myc/Max/Mad family dimers and the competition for dimerization in living cells. *Mol Cell Biol*. 2004; 24:4294–308. [PubMed: 15121849]
40. Michnick SW, Ear PH, Manderson EN, Remy I, Stefan E. Universal strategies in research and drug discovery based on protein-fragment complementation assays. *Nat Rev Drug Discov*. 2007; 6:569–82. [PubMed: 17599086]
41. Chu J, et al. A novel far-red bimolecular fluorescence complementation system that allows for efficient visualization of protein interactions under physiological conditions. *Biosens Bioelectron*. 2009; 25:234–9. [PubMed: 19596565]
42. Altman D, Goswami D, Hasson T, Spudich JA, Mayor S. Precise positioning of myosin VI on endocytic vesicles in vivo. *PLoS Biol*. 2007; 5:e210. [PubMed: 17683200]
43. Sharma P, et al. Nanoscale organization of multiple GPI-anchored proteins in living cell membranes. *Cell*. 2004; 116:577–89. [PubMed: 14980224]
44. Varma R, Mayor S. GPI-anchored proteins are organized in submicron domains at the cell surface. *Nature*. 1998; 394:798–801. [PubMed: 9723621]
45. Jares-Erijman EA, Jovin TM. FRET imaging. *Nat Biotechnol*. 2003; 21:1387–95. [PubMed: 14595367]
46. Jares-Erijman EA, Jovin TM. Imaging molecular interactions in living cells by FRET microscopy. *Curr Opin Chem Biol*. 2006; 10:409–16. [PubMed: 16949332]
47. Wallrabe H, Periasamy A. Imaging protein molecules using FRET and FLIM microscopy. *Curr Opin Biotechnol*. 2005; 16:19–27. [PubMed: 15722011]
48. Peyker A, Rocks O, Bastiaens PI. Imaging activation of two Ras isoforms simultaneously in a single cell. *Chembiochem*. 2005; 6:78–85. [PubMed: 15637661]
49. Murakoshi H, Lee SJ, Yasuda R. Highly sensitive and quantitative FRET-FLIM imaging in single dendritic spines using improved non-radiative YFP. *Brain Cell Biol*. 2008; 36:31–42. [PubMed: 18512154]

50. Kwok S, et al. Genetically encoded probe for fluorescence lifetime imaging of CaMKII activity. *Biochem Biophys Res Commun.* 2008; 369:519–25. [PubMed: 18302935]
51. Kremers GJ, van Munster EB, Goedhart J, Gadella TW Jr. Quantitative lifetime unmixing of multiexponentially decaying fluorophores using single-frequency fluorescence lifetime imaging microscopy. *Biophys J.* 2008; 95:378–89. [PubMed: 18359789]
52. Goedhart J, Vermeer JE, Adjobo-Hermans MJ, van Weeren L, Gadella TW Jr. Sensitive detection of p65 homodimers using red-shifted and fluorescent protein-based FRET couples. *PLoS One.* 2007; 2:e1011. [PubMed: 17925859]
53. Shcherbo D, et al. Practical and reliable FRET/FLIM pair of fluorescent proteins. *BMC Biotechnol.* 2009; 9:24. [PubMed: 19321010]
54. Padilla-Parra S, et al. Quantitative comparison of different fluorescent protein couples for fast FRET-FLIM acquisition. *Biophys J.* 2009; 97:2368–76. [PubMed: 19843469]
55. Pertz O, Hodgson L, Klemke RL, Hahn KM. Spatiotemporal dynamics of RhoA activity in migrating cells. *Nature.* 2006; 440:1069–72. [PubMed: 16547516]
56. Nalbant P, Hodgson L, Kraynov V, Touthkine A, Hahn KM. Activation of endogenous Cdc42 visualized in living cells. *Science (New York, NY).* 2004; 305:1615–1619.
57. Kraynov VS, et al. Localized Rac activation dynamics visualized in living cells. *Science.* 2000; 290:333–7. [PubMed: 11030651]
58. Berlin JR, Bassani JW, Bers DM. Intrinsic cytosolic calcium buffering properties of single rat cardiac myocytes. *Biophys J.* 1994; 67:1775–87. [PubMed: 7819510]
59. Helmchen F, Imoto K, Sakmann B. Ca²⁺ buffering and action potential-evoked Ca²⁺ signaling in dendrites of pyramidal neurons. *Biophys J.* 1996; 70:1069–81. [PubMed: 8789126]
60. Mochizuki N, et al. Spatio-temporal images of growth-factor-induced activation of Ras and Rap1. *Nature.* 2001; 411:1065–8. [PubMed: 11429608]
61. Sawano A, Takayama S, Matsuda M, Miyawaki A. Lateral propagation of EGF signaling after local stimulation is dependent on receptor density. *Dev Cell.* 2002; 3:245–57. [PubMed: 12194855]
62. O'Rourke NA, Meyer T, Chandy G. Protein localization studies in the age of 'Omics'. *Curr Opin Chem Biol.* 2005; 9:82–7. [PubMed: 15701458]
63. Schultz C, Schleifenbaum A, Goedhart J, Gadella TW Jr. Multiparameter imaging for the analysis of intracellular signaling. *Chembiochem.* 2005; 6:1323–30. [PubMed: 16010697]
64. Miyawaki A. Visualization of the spatial and temporal dynamics of intracellular signaling. *Developmental Cell.* 2003; 4:295–305. [PubMed: 12636912]
65. Bakal C, Aach J, Church G, Perrimon N. Quantitative morphological signatures define local signaling networks regulating cell morphology. *Science.* 2007; 316:1753–1756. [PubMed: 17588932]
66. Machacek M, Danuser G. Morphodynamic profiling of protrusion phenotypes. *Biophysical Journal.* 2006; 90:1439–1452. [PubMed: 16326902]
67. Taylor RJ, et al. Dynamic analysis of MAPK signaling using a high-throughput microfluidic single-cell imaging platform. *Proceedings of the National Academy of Sciences of the United States of America.* 2009; 106:3758–3763. [PubMed: 19223588]
68. Kiosses WB, Shattil SJ, Pampori N, Schwartz MA. Rac recruits high-affinity integrin α v β 3 to lamellipodia in endothelial cell migration. *Nat Cell Biol.* 2001; 3:316–20. [PubMed: 11231584]
69. Wang Y, et al. Visualizing the mechanical activation of Src. *Nature.* 2005; 434:1040–1045. [PubMed: 15846350]
70. Levskaya A, Weiner OD, Lim WA, Voigt CA. Spatiotemporal control of cell signalling using a light-switchable protein interaction. *Nature.* 2009; 461:997–1001. [PubMed: 19749742]
71. Wu YI, et al. A genetically encoded photoactivatable Rac controls the motility of living cells. *Nature.* 2009; 461:104–8. [PubMed: 19693014]
72. Tkachenko E, et al. Protein Kinase A Governs a RhoA-RhoGDI-driven Protrusion-Retraktion Pacemaker in Migrating Cells. *Nature Cell Biol.* In Press.
73. Locasale JW, Wolf-Yadlin A. Maximum Entropy Reconstructions of Dynamic Signaling Networks from Quantitative Proteomics Data. *Plos One.* 2009; 4

74. Perrin BE, et al. Gene networks inference using dynamic Bayesian networks. *Bioinformatics*. 2003; 19:II138–II148. [PubMed: 14534183]
75. Sachs K, et al. Learning Signaling Network Structures with Sparsely Distributed Data. *Journal of Computational Biology*. 2009; 16:201–212. [PubMed: 19193145]
76. Gulyani A, et al. A biosensor generated via high-throughput screening quantifies cell edge Src dynamics. *Nature Chemical Biology*. 2011 In Press.
77. Galperin E, Verkhusha VV, Sorkin A. Three-chromophore FRET microscopy to analyze multiprotein interactions in living cells. *Nat Methods*. 2004; 1:209–17. [PubMed: 15782196]
78. He L, Wu X, Simone J, Hewgill D, Lipsky PE. Determination of tumor necrosis factor receptor-associated factor trimerization in living cells by CFP->YFP->mRFP FRET detected by flow cytometry. *Nucleic Acids Res*. 2005; 33:e61. [PubMed: 15805120]
79. Wu X, et al. Measurement of two caspase activities simultaneously in living cells by a novel dual FRET fluorescent indicator probe. *Cytometry A*. 2006; 69:477–86. [PubMed: 16683263]
80. Kawai H, et al. Simultaneous imaging of initiator/effector caspase activity and mitochondrial membrane potential during cell death in living HeLa cells. *Biochim Biophys Acta*. 2004; 1693:101–10. [PubMed: 15313012]
81. Kawai H, et al. Simultaneous real-time detection of initiator- and effector-caspase activation by double fluorescence resonance energy transfer analysis. *J Pharmacol Sci*. 2005; 97:361–8. [PubMed: 15750288]
82. DiPilato LM, Cheng X, Zhang J. Fluorescent indicators of cAMP and Epac activation reveal differential dynamics of cAMP signaling within discrete subcellular compartments. *Proc Natl Acad Sci U S A*. 2004; 101:16513–8. [PubMed: 15545605]
83. Brumbaugh J, Schleifenbaum A, Gasch A, Sattler M, Schultz C. A dual parameter FRET probe for measuring PKC and PKA activity in living cells. *J Am Chem Soc*. 2006; 128:24–5. [PubMed: 16390103]
84. Ouyang M, et al. Simultaneous visualization of protumorigenic Src and MT1-MMP activities with fluorescence resonance energy transfer. *Cancer Res*. 2010; 70:2204–12. [PubMed: 20197470]
85. Grant DM, et al. Multiplexed FRET to image multiple signaling events in live cells. *Biophys J*. 2008; 95:L69–71. [PubMed: 18757561]

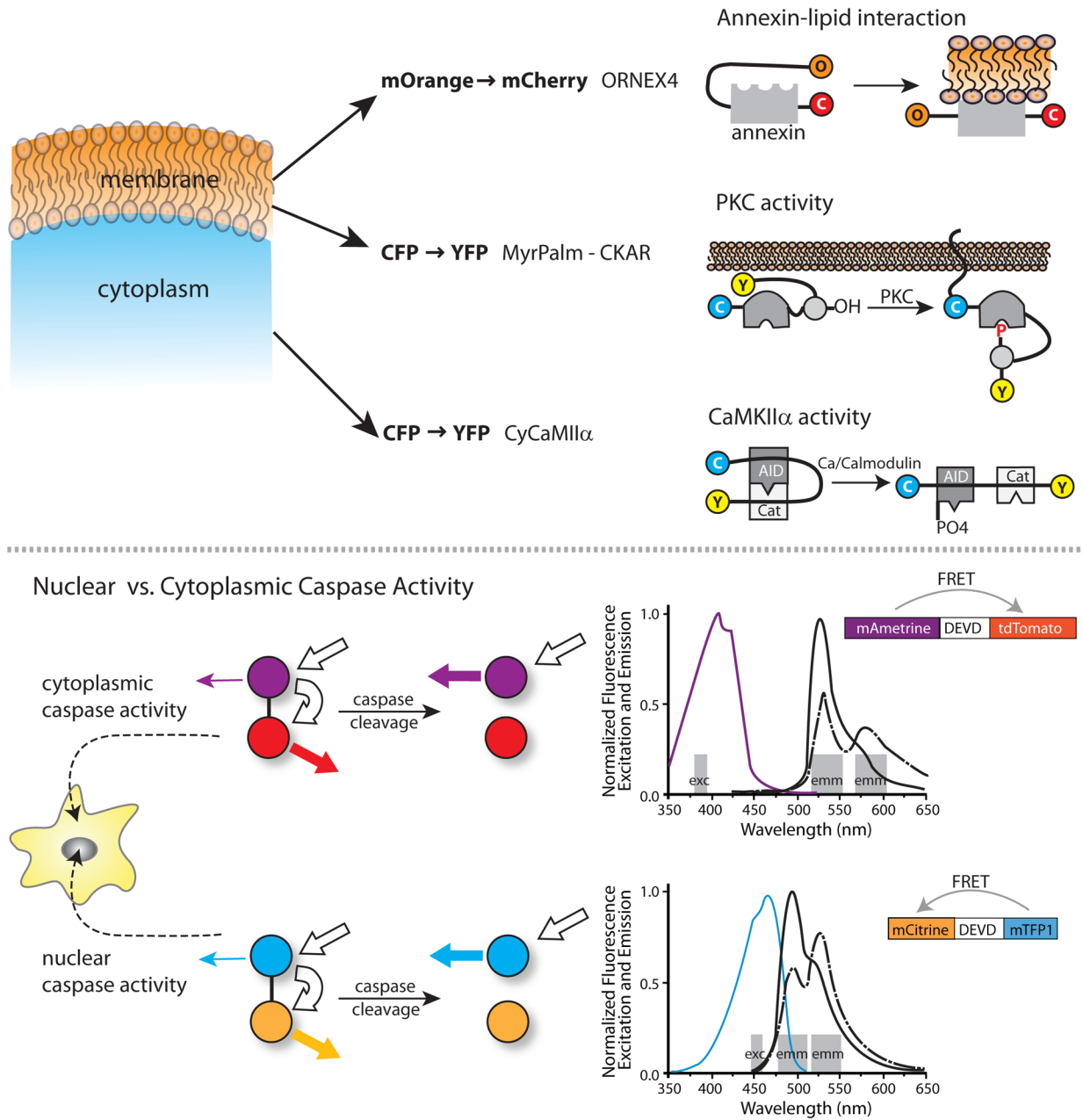


Figure 1. Examples of Experimental Multiplexing

Top) Pilijik and Schultz discriminate signals from three biosensors by using both orthogonal FRET pairs and differences in subcellular localization. They examine the relative kinetics of lipid modification, PCK activity and Cam Kinase IIa activity by using a biosensor with mOrange to mCherry FRET, combined with two biosensors using CFP to YFP FRET. One CFP to YFP biosensor is restricted to the cytosol and the other to the plasma membrane. Bottom) Ai et al. developed a novel fluorescent protein, mAmetrine, with an unusually large Stokes shift. This facilitated separation of wavelengths to image two biosensors independently in the same cell. The Stokes shift enabled fluorophore excitation and monitoring of emission at the orthogonal wavelength bands shown by the grey bars. For each FRET pair a single excitation band is used, leading to emission due to either direct excitation of the donor (mAmetrine or mTFP) or FRET emission from the acceptor (mTomato

or mTFP). Excitation and emission spectra are shown for the FRET pair in each biosensor, with the color of the excitation spectra corresponding to the donor fluorophores in the biosensors. Bold white arrows show the excitation and FRET of the donor fluorophore, while the colored arrows show the level of emission from the acceptors before and after cleavage. These orthogonal FRET biosensors were used to differentiate caspase activities monitored simultaneously in the nucleus and cytoplasm.

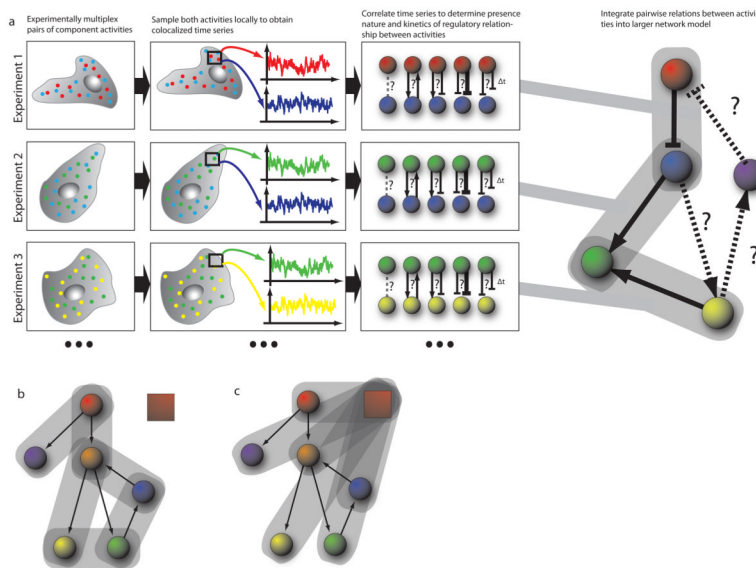


Figure 2. Workflow of Computational Multiplexing

a) In each experiment, a sub-set of the signaling network components (‘nodes’) are experimentally multiplexed (two in the illustrated example). Component activities are sampled locally to extract co-localized time-series for each experimentally multiplexed node, in each region of the cell. The sampling windows are defined in a cell-centered frame of reference (see Fig. 4) in order to generate time series that are independent of the cell-cell to variation in shape. These time series are then analyzed by correlation methods, testing first the presence of an interaction between the activities and then determining the direction and sign (stimulating or inhibiting) as well as the timing of the interaction. This process is repeated for other activity pairs in the network, with each subsequent experiment sharing a common node with any of the previous experiments – that is in this illustration experiments 1 and 2 share observations from the blue node, while experiments 2 and 3 share observations from the green node. Continuing this process allows traversal of the network, without requiring each node to be observed simultaneously. Mathematical tools allow integration of the pairwise and possibly redundant observations into a larger network model. **b, c)** Two strategies for traversing the network. Experiment establishes pairwise relations between activities throughout the network, **b)**; or each experiment established the relation of one activities relative to a common fiduciary activity, depicted by red box, **c)**.

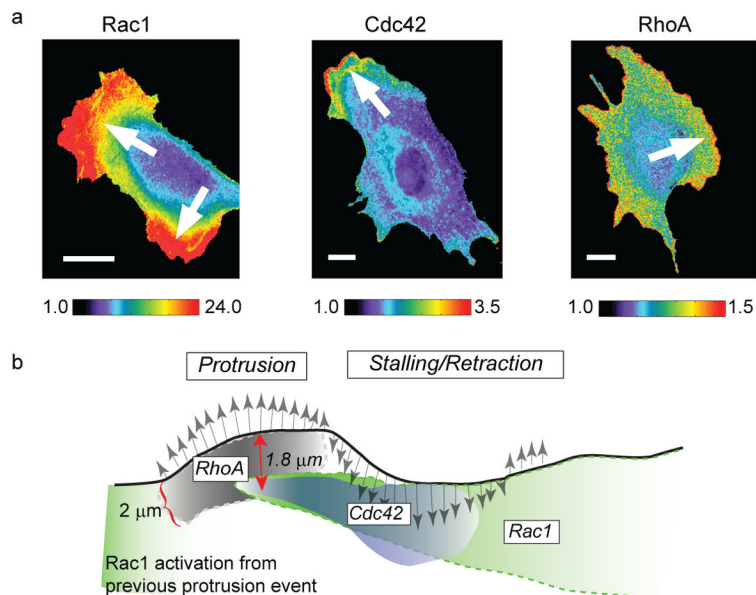


Figure 3. Assessing the activity of Rho GTPases using computational multiplexing

a) Three distinct members of the family of Rho GTPases (Rac1, Cdc42 and RhoA) were imaged in different cells using different biosensors. To monitor Rac1 activation, a bimolecular FRET reporter was used, which produces a high signal when a Rac-binding fragment of the Rac1-effector Pak conjugated to cyPet associates the activated form of Rac1 conjugated to YPet. To monitor Cdc42 activation, an environmentally-sensitive dye, mero87, was coupled to a Cdc42-binding fragment of the Cdc42-effector WASP. Upon association of this labeled fragment with the activated form of Cdc42 the dye undergoes a change in its fluorescence spectrum that is observed as a strong increase in fluorescence at a particular wavelength. To monitor RhoA activation, an intramolecular FRET reporter was used. In contrast to the Rac1 reporter, here RhoA and the RhoA-binding fragment are in a single chain, which undergoes conformational changes upon activation of RhoA. These changes are detected by changes in the FRET intensity between cyPet-/YPet-fluorescent proteins inserted into the single chain sensor. Pseudo-color scales indicate the dynamic range of the biosensor responses (1, no significant response; maximum value, strongest response throughout the time-lapse sequence). Arrows indicate the direction of cell protrusion. **b)** Cartoon illustrating the spatially and temporally differentiated activation of the three Rho GTPases during protrusion (gray arrows pointing north) and retraction/stalling (gray arrows pointing south) events at the cell edge. The shading in the activation clouds indicates how the signaling strength decreases after initial induction. The relations between the signaling activities were predicted first indirectly by spatiotemporal cross-correlation analysis of each biosensor in a separate cell to the velocity of edge movement as a common fiduciary (strategy Fig. 2c). The inferred relations were then confirmed by direct observation of two of the biosensors (Cdc42 and RhoA) in the same cell (strategy Fig. 2b). Images reproduced from²² with permission from Nature.

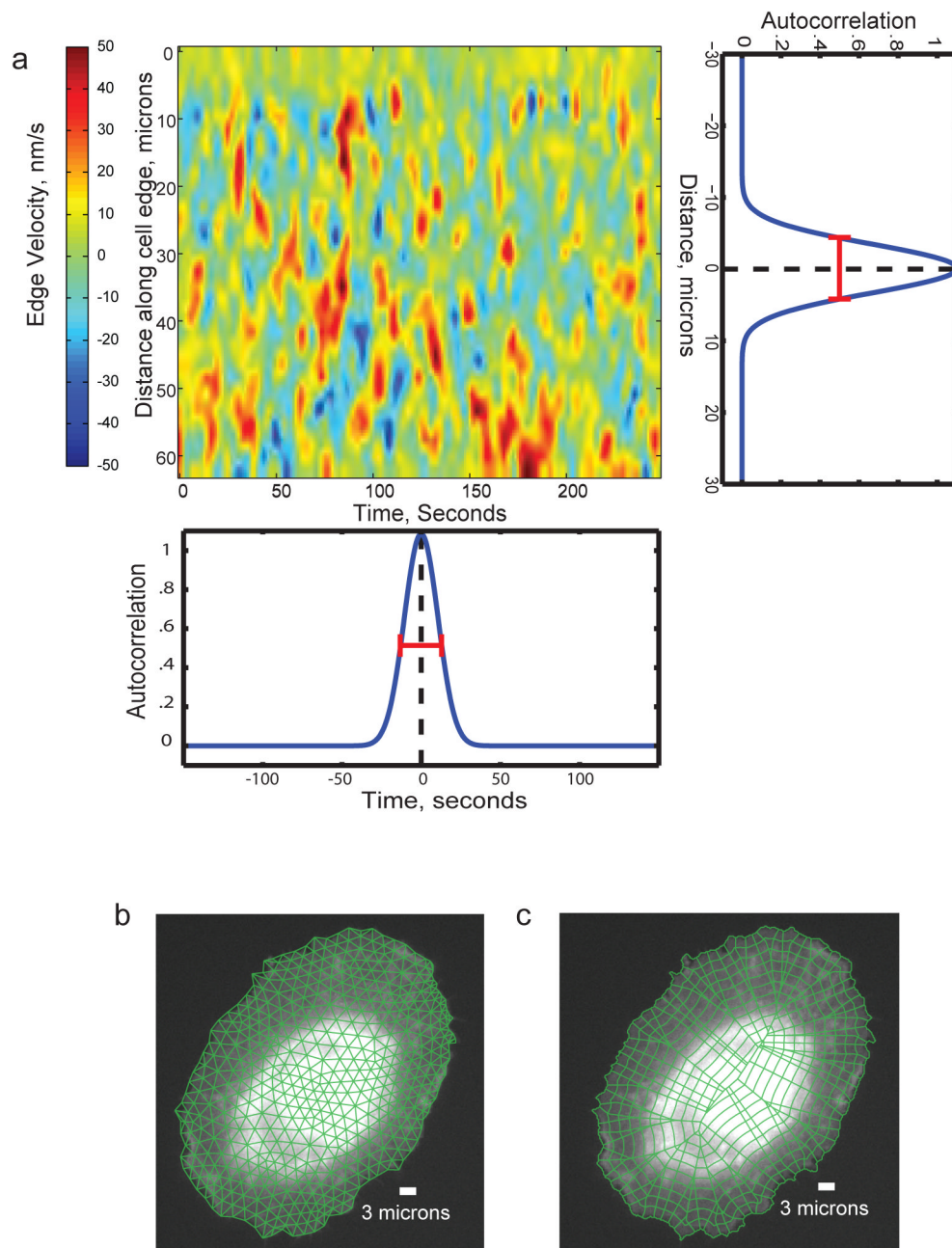


Figure 4. Determining the requirements for spatiotemporal sampling to allow computational multiplexing based on constitutive fluctuations

a) Map of the spatial (vertical axis) and temporal (horizontal axis) activity of an experimental fiduciary (here cell edge velocity). The activity map displays typical stochastic oscillations, as seen for many cellular activities. The horizontal autocorrelation of the map indicates the characteristic time scale of the oscillations (~ 40 s in this example, as deduced from the full width at half maximum (FWHM) of the function, red bar). This time scale defines the requirement for temporal sampling. The vertical autocorrelation of the map indicates the characteristic length scale of the oscillations (~ 15 μm in this example, as deduced from the FWHM). This length scale defines the requirement for spatial sampling. For both, time and space domain 2 – 4 fold oversampling should be achieved. That is,

movies should be acquired at 10 s frame intervals or faster and biosensor intensities should be sampled in probing windows of max. 4 microns side length. **b)** Definition of a triangular mesh of appropriately-sized probing windows. **c)** Definition of a polygonal mesh of appropriately-sized probing windows. In contrast to the triangular mesh in b), each window inside the cell perimeter has a unique relation to a window at the cell periphery. Thus, this mode of windowing is preferred for studies that relate intracellular signals to cell protrusion and retraction events.